

Quantum metrology at the limit with extremal Majorana constellations

F. BOUCHARD¹, P. DE LA HOZ², G. BJÖRK³, R. W. BOYD^{1,4}, M. GRASSL⁵,
Z. HRADIL⁶, E. KARIMI^{1,7,*}, A. B. KLIMOV⁸, G. LEUCHS^{5,1}, J. ŘEHÁČEK⁶, AND
L. L. SÁNCHEZ-SOTO^{2,5}

¹Department of Physics, University of Ottawa, 150 Louis Pasteur, Ottawa, Ontario, K1N 6N5 Canada

²Department of Optics, Faculty of Physics, Universidad Complutense, 28040 Madrid, Spain

³Department of Applied Physics, Royal Institute of Technology (KTH), AlbaNova, SE-106 91 Stockholm, Sweden

⁴Institute of Optics, University of Rochester, Rochester, New York, 14627, USA

⁵Max Planck Institute for the Science of Light, Staudtstraße 2, 91058 Erlangen, Germany

⁶Department of Optics, Palacký University, 17. listopadu 12, 771 46 Olomouc, Czech Republic

⁷Department of Physics, Institute for Advanced Studies in Basic Sciences, 45137-66731 Zanjan, Iran

⁸Department of Physics, Universidad de Guadalajara, 44420 Guadalajara, Jalisco, Mexico

*Corresponding author: ekarimi@uottawa.ca

Compiled November 28, 2021

Quantum metrology allows for a tremendous boost in the accuracy of measurement of diverse physical parameters. The estimation of a rotation constitutes a remarkable example of this quantum-enhanced precision. The recently introduced Kings of Quantumness are especially germane for this task when the rotation axis is unknown, as they have a sensitivity independent of that axis and they achieve a Heisenberg-limit scaling. Here, we report the experimental realization of these states by generating up to 21-dimensional orbital angular momentum states of single photons, and confirm their high metrological abilities.

© 2016 Optical Society of America

OCIS codes: (270.0270) Quantum optics; (270.5585) Quantum information and processing; (120.3940) Metrology.

<http://dx.doi.org/10.1364/aop.XX.XXXXXX>

The conventional description of the quantum world involves a key mathematical object—the quantum state—that conveys complete information about the system under study: once it is known, the probabilities of the outcomes of any measurement can be predicted. This statistical description entails counterintuitive effects that have prompted several notions of quantumness, yet no single one captures the whole breadth of the physics.

There are, however, instances of quantum states that behave in an almost classical way. The paradigm of such a behavior is

that of coherent states of light [1]: they are as much localized as possible in phase space, a property that is preserved under free evolution.

The concept of coherent states has been extended to other physical systems [2]. The case of a spin is of paramount importance. The corresponding spin coherent states have minimal uncertainty and they are conserved under rotations. So, in the usual way of speaking, they mimic a classical angular momentum as much as possible. One could rightly wonder what kind of state might serve as the opposite of a coherent state. The answer will depend on the ways to formalize the idea of being “the opposite” [3]. Here, we take advantage of the Majorana representation, which maps a pure spin S into $2S$ points on the Bloch sphere [4].

It turns out that the Majorana representation of a coherent state consists of a single point (with multiplicity $2S$). At the opposite extreme, we can imagine states whose Majorana representations are spread uniformly over the sphere. The resulting states are precisely the Kings of Quantumness [5, 6]. With such symmetric spreadings, the constellations essentially map onto themselves for relatively small rotations around arbitrary axes. This means that they resolve rotations around any axis approximately equally well. We emphasize that the problem of estimating a rotation is of utmost interest in magnetometry [7–9], polarimetry [10, 11], and metrology in general [12]. In this work, we experimentally demonstrate the generation of these states and certify their potential for quantum metrology [13].

Let us first set the stage for our experiment. We consider a system that can be described in terms of two independent bosonic modes, with creation operators \hat{a}_α^\dagger , with $\alpha \in \{+, -\}$. This encompasses many different instances, such as strongly correlated systems, light polarization, Bose-Einstein condensates, and Gaussian-Schell beams, to mention only but a few [14].

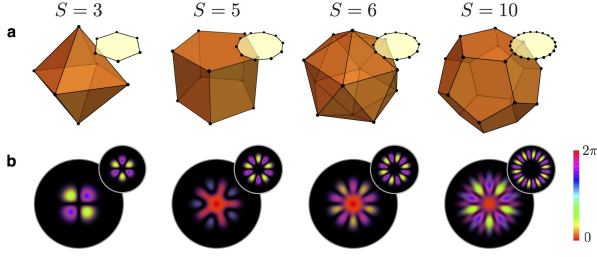


Fig. 1. (a) The Majorana constellations in the Bloch sphere for the Kings (orange) and the NOON states (yellow) corresponding to spin $S = 3, 5, 6$, and 10 . (b) The Laguerre-Gauss representation of the same Kings and NOON states, shown in (a), where the azimuthal index ℓ corresponds to m in the Dicke basis. We consider the fundamental radial mode; i.e., $p = 0$, where p is the radial index of the Laguerre-Gauss modes.

The Stokes operators for these two-mode systems can be compactly expressed as [15] $\hat{\mathbf{S}} = \frac{1}{2}\hat{a}_\alpha^\dagger \sigma_{\alpha\beta} \hat{a}_\beta$, where σ denote the Pauli matrices and summation over repeated indices is assumed. One can verify that $\hat{\mathbf{S}}^2 = \hat{S}_0(\hat{S}_0 + \mathbf{1})$, with $\hat{S}_0 = \hat{N}/2$ and $\hat{N} = \hat{a}_\alpha^\dagger \delta_{\alpha\beta} \hat{a}_\beta = \hat{N}_+ + \hat{N}_-$ being the total number of excitations.

From now on, we restrict our attention to the case where N is fixed. This corresponds to working in a $(2S + 1)$ -dimensional Hilbert space \mathcal{H}_S of spin S (with $N = 2S$). This space \mathcal{H}_S is spanned by the Dicke basis $|S, m\rangle$, wherein the action of $\hat{\mathbf{S}}$ operators is the standard for an angular momentum. Sometimes, it is preferable to use the two-mode Fock basis $|N_+, N_- \rangle$; related to the Dicke basis by $N_+ = S + m$ and $N_- = S - m$.

Spin coherent states are constructed much in the same way as in the canonical case [2]: they are displaced versions of the north pole of the Bloch unit sphere S_2 . If \mathbf{n} is a unit vector in the direction of the spherical angles (θ, ϕ) , they can be defined as $|\mathbf{n}\rangle = e^{i\phi\hat{S}_z} e^{i\theta\hat{S}_y} |S, S\rangle$. They are not orthogonal, but one can still decompose an arbitrary state $|\Psi\rangle$ using this overcomplete set. The associated coherent-state wave function is $\Psi(\mathbf{n}) = \langle \mathbf{n} | \Psi \rangle$, and the corresponding probability distribution, $Q(\mathbf{n}) = |\Psi(\mathbf{n})|^2$, is nothing but the Husimi function.

The wave function $\Psi(\mathbf{n})$ can be expanded in terms of the Dicke basis $|S, m\rangle$. If the corresponding coefficients are $\Psi_m = \langle S, m | \Psi \rangle$, we obtain $\Psi(\mathbf{n}) = (1 + |z|^2)^{-S} \sum_{m=-S}^S c_m \Psi_m z^{S+m}$, where $c_m = \sqrt{(2S)! / [(S-m)!(S+m)!]}$ and $z = \tan(\theta/2)e^{-i\phi}$ is the complex number derived by the stereographic projection of (θ, ϕ) . Apart from the unessential positive prefactor, this is a polynomial of order $2S$; thus, $|\Psi\rangle$ is determined by the set $\{z_i\}$ of the $2S$ complex zeros of $\Psi(\mathbf{n})$. These zeros, which are also the zeros of $Q(\mathbf{n})$, specify the so-called constellation by an inverse stereographic map of $\{z_i\} \mapsto (\theta_i, \phi_i)$.

Since the spherical harmonics $Y_{Kq}(\mathbf{n})$ are a complete set of orthonormal functions on S_2 , they may be used to expand the Husimi function $Q(\mathbf{n})$. The resulting coefficients, q_{Kq} , are nothing but the standard state multipoles [16] and there are $2S + 1$ of them (see Supplemental material). The monopole is trivial, as it is just a constant term. The dipole indicates the position of the state in the Bloch sphere. When it vanishes, the state has vanishing (first-order) polarization and points nowhere in the mean. If the quadrupole also vanishes, the variance of the state is uniform; i.e., no directional signature can be observed in its second-order fluctuations and we say that it is second-order unpolarized. Similar interpretation holds for higher-order multipoles. One can also look at these multipoles as the K th

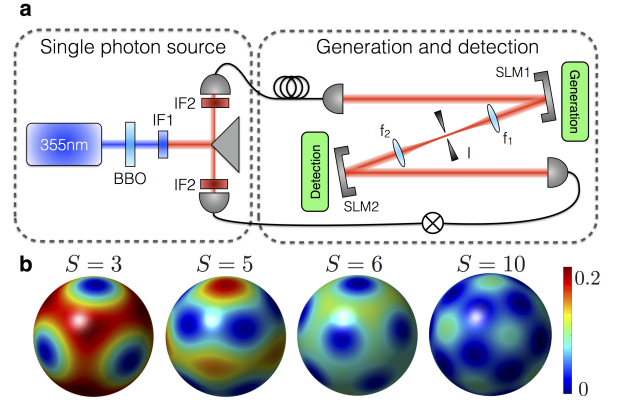


Fig. 2. (a) Sketch of the experimental setup and (b) density plots of the experimentally reconstructed Husimi Q functions for the same King states as in Fig. 1. The fidelities of these reconstructed states are (from left to right) 0.94, 0.87, 0.91, and 0.93. The differences with the theoretical Q functions cannot be visually noticed.

directional moments of the state constellation and, therefore, these terms resolve progressively finer angular features.

The quantity $\sum_q |q_{Kq}|^2$ gauges the overlap of the state with the K th multipole pattern. It seems thus suitable to look at the cumulative distribution [17] $\mathcal{A}_M = \sum_{K=1}^M \sum_{q=-K}^K |q_{Kq}|^2$, which concisely condenses the state angular capacity up to order M ($1 \leq M \leq 2S$). Observe that the monopole is omitted, as it is just a constant term.

The spin coherent states $|\mathbf{n}\rangle$ have remarkably simple constellations, just the point $-\mathbf{n}$, and maximize \mathcal{A}_M for all orders M , confirming yet from another perspective the outstanding properties of these states [5].

In contradistinction, the Kings are those pure states that make $\mathcal{A}_M \equiv 0$ for the highest possible value of M . This means that they convey the relevant information in higher-order fluctuations. The search for these states has been systematically undertaken recently in Ref. [5], where the interested reader can check the details (see also Supplemental Material, where one can find the nonzero components Ψ_m of the Kings). The resulting Majorana constellations for some values of S are depicted in Fig. 1. For $S = 3$, the constellation is a regular octahedron and the state is third-order unpolarized ($M = 3$). For $S = 5$, it consists of two pentagons. For $S = 6$ we have the icosahedron, and the corresponding state is fifth-order unpolarized. For $S = 10$ we have a slightly stretched dodecahedron (i.e., the four pentagonal rings that define its vertices are displaced against the pole) and it is fifth-order unpolarized. As we can appreciate, the Kings have the points very symmetrically placed on the unit sphere, so their constellations possess many axes along which they return to themselves after a rotation. Consequently, they can resolve relatively small angles around a large number of axes.

Other states with a high degree of angular resolution are the NOON states, given by $|\text{NOON}\rangle = \frac{1}{\sqrt{2}}(|N, 0\rangle - |0, N\rangle)$ in the two-mode Fock basis and $\frac{1}{\sqrt{2}}(|S, S\rangle - |S, -S\rangle)$ in the Dicke basis. As shown in Fig. 1 their Majorana constellation consists of $2S$ equidistantly placed points around the equator of S_2 . A rotation around the z axis of angle $\pi/(2S)$ makes $|\text{NOON}\rangle$ orthogonal to itself, whereas for π/S it returns to itself. This nicely supports the ability of NOON states to detect small rotations.

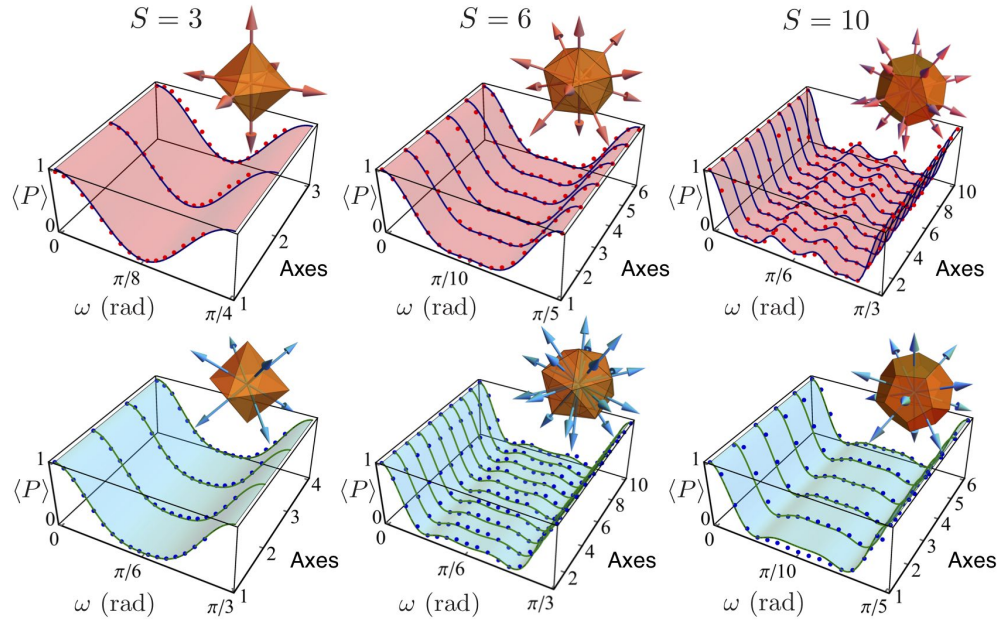


Fig. 3. Experimental results of the projection of the $S = 3, 6$ and 10 (first, second, and third column, respectively) Kings states, $|\Psi^{(S)}\rangle$, onto themselves after a rotation of ω around the axis \mathbf{u} , $\hat{R}(\omega, \mathbf{u})$; i.e., $\langle \hat{P} \rangle = |\langle \Psi^{(S)} | \hat{R}(\omega, \mathbf{u}) | \Psi^{(S)} \rangle|^2$. The axes are presented graphically along with the associated constellations. The first row corresponds to rotations along the axes passing through the Majorana points (pink arrows) and the second row corresponds to rotations along the axes normal to the facets of the constellations (blue arrows). The experimental results (red and blue dots) are shown along with the theoretical results (blue and green curves) for all rotation axes.

To compare the performance of these two classes of states, let us assume we have to estimate a rotation $R(\omega, \mathbf{u})$ of angle ω around an axis \mathbf{u} of spherical angles (Θ, Φ) . We consider only small rotations and take the measurement to be a projection of the rotated state onto the original one; i.e., it can be represented by $\hat{P} = |\Psi\rangle\langle\Psi|$. As discussed in the Supplemental material, the respective sensitivities (defined as the ratio $\Delta\omega = \Delta\hat{P}/|\partial\langle\hat{P}\rangle/\partial\omega|$, the variance being $\Delta\hat{P} = [\langle\hat{P}^2\rangle - \langle\hat{P}\rangle^2]^{1/2}$) are

$$\begin{aligned} \Delta\omega_{\text{Kings}} &= \frac{\sqrt{3}}{2} \frac{1}{\sqrt{S(S+1)}}, \\ \Delta\omega_{\text{NOON}} &= \frac{1}{\sqrt{2}} \frac{1}{\sqrt{2S^2 \cos^2 \Theta + S \sin^2 \Theta}}. \end{aligned} \quad (1)$$

The sensitivity of the Kings is completely independent of the rotation axis and with a Heisenberg-limit scaling $1/S$ for large S . For the NOON states, the sensitivity scales as $1/S$ when $\Theta = 0$, but can be as bad as $1/\sqrt{S}$ when $\Theta = \pi/2$. In short, it is essential to know the rotation axis to ensure that the NOON state is aligned to achieve its best sensitivity.

We stress that the measurement scheme for $\Delta\omega$ involves only second-order moments of $\hat{\mathbf{S}}$. Given their properties, one could expect that detecting higher-order moments will bring out even more advantages of the Kings.

To check these issues we have generated these extremal states for the cases of $S = 3, 5, 6$ and 10 , using orbital angular momentum (OAM) states of single photons [18], which has already proven fruitful in quantum metrology [19]. Working at the single-photon regime is not essential, but it highlights the potential implications for quantum information processing [20]. Therefore, the index m in the Dicke basis is identified with the OAM eigenvalue ℓ of a single photon along its propagation direction. In general, there exist many families of optical modes

carrying OAM, but we choose the Laguerre-Gauss basis $\text{LG}_{\ell,p}$, where p is the radial index. Since the radial profile is irrelevant to the experimental realization of the Kings states, for the sake of simplicity, we always set the radial index to its fundamental value, i. e. $p = 0$. The resulting transverse profiles of both the Kings and the NOON states are as in Fig. 1(b).

We experimentally create the Kings by means of spontaneous parametric downconversion. A sketch of the experimental setup is shown in Fig. 2(a). A quasi-continuous wave UV laser operating with a repetition rate of 100 MHz and an average power of 150 mW at a wavelength of 355 nm is used to pump a type-I β -barium borate crystal. The single photons, signal and idler, are subsequently coupled to single mode fibres to filter their spatial mode. One of the photons, the idler, is used as a trigger. The other photon, the signal, is made incident on a first spatial light modulator (SLM1), where the desired quantum states were imprinted on the signal photon holographically [21]. The generated photonic Kings are subsequently imaged onto a second spatial light modulator (SLM2) by a $4f$ system. The second SLM possessing the desired hologram followed by a single mode optical fibre perform the projective measurement on the state of the signal photon. Both photons are sent to avalanche photodiode detectors (APD) and coincidence counts are recorded by a coincidence box with a coincidence time window of 3 ns [22].

To verify the accurate experimental generation of these states, we perform quantum state tomography to reconstruct the Husimi Q function, as shown in Fig. 2(b). The average fidelity of the resulting states is above 90%; i.e., 94%, 87%, 91% and 93%, respectively (see Supplemental Material).

We now study the behaviour of such states under rotations in the sphere S_2 . This is experimentally realized by projective measurements of the Kings onto themselves after a rotation

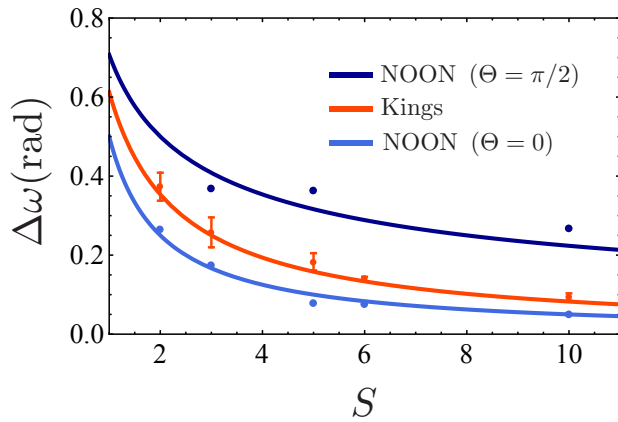


Fig. 4. Rotational sensitivity $\Delta\omega$ for the Kings (red) and NOON states (blue). The solid curves correspond to the theory predicted in Eq. (1) and the points correspond to experimental results. In the case of the Kings, we show the mean rotational sensitivity over all axes presented in Fig. 3, where the error bars correspond to variation in sensitivity from axes to axes. For the NOON states, we show the rotational sensitivity for rotation axes with $\Theta = 0$ and $\Theta = \pi/2$.

ω around several axes (see Fig. 3). To demonstrate the high sensitivity to rotation of these states along arbitrary axes, we perform such rotations around each axis passing through the Majorana points, and facets of the Kings constellations. For the cases of $S = 3, 6$ and 10 , we find four-, five- and three-fold symmetry axes passing through their Majorana points and three-, three- and five-fold symmetry axes passing through the normals to the facets of their constellations, respectively. Note that, since we are dealing with OAM, these rotations correspond to rather abstract mode transformations, although the polar axis still represent a physical real-space rotation around the optical axis.

Finally, in Fig. 4 we experimentally check the sensitivity of the Kings and NOON states. As we can see, the experimental sensitivity of the Kings is completely independent of the orientation of the rotation axes (within the error bars). In the limit of small rotation angles, the NOON states overcome the Kings all the way up to $\cos \Theta = 1/\sqrt{3}$. Nonetheless, since the Kings achieve the ideal sensitivity irrespectively of the axis, they are the most appropriate to detect rotation around arbitrary axes.

The problem of the Kings is closely related to other notions as states of maximal Wehrl-Lieb entropy [23], Platonic states [24], the Queens of Quantumness [25] or the Thomson problem [26]. However, there are still many things to elucidate concerning these links. They are though a nice illustration of the connections between different branches of science, and on how some seemingly simple problems—distributing points in the most symmetric manner on a sphere—can illuminate such complicated optimization problems that we have just described.

Thus far, efforts were concentrated in estimating the rotation angle, which in terms of magnetometry means that we only want to know the magnetic field magnitude. The Kings will allow for a simultaneous precise determination of the rotation axis (i.e., the magnetic field direction). Our experimental results corroborate that this extra advantage can pave the way to much more refined measurement schemes.

FUNDING INFORMATION

F. B. acknowledges the support of the Vanier Canada Graduate Scholarships Program of the Natural Sciences and Engineering Research Council of Canada (NSERC). E. K. acknowledges the support of the Canada Research Chairs (CRC), and Canada Foundation for Innovation (CFI) Programs. F. B., R. W. B and E. K. acknowledge the support of the Max Planck–University of Ottawa Centre for Extreme and Quantum Photonics. Z. H. and J. R. acknowledge the support from the Technology Agency of the Czech Republic (Grant TE01020229), the Grant Agency of the Czech Republic (Grant 15-03194S). P. H. and L. L. S. S. acknowledges the support of the Spanish MINECO (Grant FIS2015-67963-P).

REFERENCES

1. R. J. Glauber, *Phys. Rev.* **131**, 2766 (1963).
2. A. Perelomov, *Generalized Coherent States and their Applications* (Springer, 1986).
3. J. Zimba, *EJTP* **3**, 143 (2006).
4. E. Majorana, *Nuovo Cimento* **9**, 43 (1932).
5. G. Björk, A. B. Klimov, P. de la Hoz, M. Grassl, G. Leuchs, and L. L. Sánchez-Soto, *Phys. Rev. A* **92**, 031801 (2015).
6. G. Björk, M. Grassl, P. de la Hoz, G. Leuchs, and L. L. Sánchez-Soto, *Physica Scripta* **90**, 108008 (2015).
7. W. Wasilewski, K. Jensen, H. Krauter, J. J. Renema, M. V. Balabas, and E. S. Polzik, *Phys. Rev. Lett.* **104**, 133601 (2010).
8. R. J. Sewell, M. Koschorreck, M. Napolitano, B. Dubost, N. Behhood, and M. W. Mitchell, *Phys. Rev. Lett.* **109**, 253605 (2012).
9. W. Muessel, H. Strobel, D. Linnemann, D. B. Hume, and M. K. Oberthaler, *Phys. Rev. Lett.* **113**, 103004 (2014).
10. V. Meyer, M. A. Rowe, D. Kielpinski, C. A. Sackett, W. M. Itano, C. Monroe, and D. J. Wineland, *Phys. Rev. Lett.* **86**, 5870 (2001).
11. V. D'Ambrosio, N. Spagnolo, L. Del Re, S. Slussarenko, Y. Li, L. C. Kwek, L. Marrucci, S. P. Walborn, L. Aolita, and F. Sciarrino, *Nat. Commun.* **4**, 2432 EP (2013).
12. L. A. Rozema, D. H. Mahler, R. Blume-Kohout, and A. M. Steinberg, *Phys. Rev. X* **4**, 041025 (2014).
13. V. Giovannetti, S. Lloyd, and L. Maccone, *Nat. Photon.* **5**, 222 (2011).
14. S. Chaturvedi, G. Marmo, and N. Mukunda, *Rev. Math. Phys.* **18**, 887 (2006).
15. A. Luis and L. L. Sánchez-Soto, *Prog. Opt.* **41**, 421 (2000).
16. K. Blum, *Density Matrix Theory and Applications* (Plenum, 1981).
17. P. de la Hoz, A. B. Klimov, G. Björk, Y. H. Kim, C. Müller, C. Marquardt, G. Leuchs, and L. L. Sánchez-Soto, *Phys. Rev. A* **88**, 063803 (2013).
18. L. Allen, S. M. Barnett, and M. J. Padgett, *Optical Angular Momentum* (Institute of Physics Publishing, 2003).
19. D. S. Simon, G. Jaeger, and A. V. Sergienko, *Quantum Metrology, Imaging, and Communication* (Springer, 2017).
20. J. Leach, M. J. Padgett, S. M. Barnett, S. Franke-Arnold, and J. Courtial, *Phys. Rev. Lett.* **88**, 257901 (2002).
21. E. Bolduc, N. Bent, E. Santamato, E. Karimi, and R. W. Boyd, *Opt. Lett.* **38**, 3546 (2013).
22. H. Qassim, F. M. Miatto, J. P. Torres, M. J. Padgett, E. Karimi, and R. W. Boyd, *J. Opt. Soc. Am. B* **31**, A20 (2014).
23. A. Baecklund and I. Bengtsson, *Phys. Scr.* **T163**, 014012 (2014).

24. P. Kolenderski and R. Demkowicz-Dobrzanski, *Phys. Rev. A* **78**, 052333 (2008).
25. O. Giraud, P. Braun, and D. Braun, *New J. Phys.* **12**, 063005 (2010).
26. J. J. Thomson, *Philos. Mag. Ser. 6* **7**, 37265 (1904).

REFERENCES

1. R. J. Glauber, "Coherent and incoherent states of the radiation field," *Phys. Rev.* **131**, 2766–2788 (1963).
2. A. Perelomov, *Generalized Coherent States and their Applications* (Springer, 1986).
3. J. Zimba, "'Anticoherent' spin states via the Majorana representation," *EJTP* **3**, 143–156 (2006).
4. E. Majorana, "Atomi orientati in campo magnetico variabile," *Nuovo Cimento* **9**, 43–50 (1932).
5. G. Björk, A. B. Klimov, P. de la Hoz, M. Grassl, G. Leuchs, and L. L. Sánchez-Soto, "Extremal quantum states and their Majorana constellations," *Phys. Rev. A* **92**, 031801 (2015).
6. G. Björk, M. Grassl, P. de la Hoz, G. Leuchs, and L. L. Sánchez-Soto, "Stars of the quantum universe: extremal constellations on the Poincaré sphere," *Physica Scripta* **90**, 108008 (2015).
7. W. Wasilewski, K. Jensen, H. Krauter, J. J. Renema, M. V. Balabas, and E. S. Polzik, "Quantum noise limited and entanglement-assisted magnetometry," *Phys. Rev. Lett.* **104**, 133601 (2010).
8. R. J. Sewell, M. Koschorreck, M. Napolitano, B. Dubost, N. Behbood, and M. W. Mitchell, "Magnetic sensitivity beyond the projection noise limit by spin squeezing," *Phys. Rev. Lett.* **109**, 253605 (2012).
9. W. Muessel, H. Strobel, D. Linnemann, D. B. Hume, and M. K. Oberthaler, "Scalable spin squeezing for quantum-enhanced magnetometry with bose-einstein condensates," *Phys. Rev. Lett.* **113**, 103004 (2014).
10. V. Meyer, M. A. Rowe, D. Kielpinski, C. A. Sackett, W. M. Itano, C. Monroe, and D. J. Wineland, "Experimental demonstration of entanglement-enhanced rotation angle estimation using trapped ions," *Phys. Rev. Lett.* **86**, 5870–5873 (2001).
11. V. D'Ambrosio, N. Spagnolo, L. Del Re, S. Slussarenko, Y. Li, L. C. Kwek, L. Marrucci, S. P. Walborn, L. Aolita, and F. Sciarrino, "Photonic polarization gears for ultra-sensitive angular measurements," *Nat. Commun.* **4**, 2432 EP (2013).
12. L. A. Rozema, D. H. Mahler, R. Blume-Kohout, and A. M. Steinberg, "Optimizing the choice of spin-squeezed states for detecting and characterizing quantum processes," *Phys. Rev. X* **4**, 041025 (2014).
13. V. Giovannetti, S. Lloyd, and L. Maccone, "Advances in quantum metrology," *Nat. Photon.* **5**, 222–229 (2011).
14. S. Chaturvedi, G. Marmo, and N. Mukunda, "The Schwinger representation of a group: concept and applications," *Rev. Math. Phys.* **18**, 887–912 (2006).
15. A. Luis and L. L. Sánchez-Soto, "Quantum phase difference, phase measurements and Stokes operators," *Prog. Opt.* **41**, 421–481 (2000).
16. K. Blum, *Density Matrix Theory and Applications* (Plenum, 1981).
17. P. de la Hoz, A. B. Klimov, G. Björk, Y. H. Kim, C. Müller, C. Marquardt, G. Leuchs, and L. L. Sánchez-Soto, "Multipolar hierarchy of efficient quantum polarization measures," *Phys. Rev. A* **88**, 063803 (2013).
18. L. Allen, S. M. Barnett, and M. J. Padgett, *Optical Angular Momentum* (Institute of Physics Publishing, 2003).
19. D. S. Simon, G. Jaeger, and A. V. Sergienko, *Quantum Metrology, Imaging, and Communication* (Springer, 2017).
20. J. Leach, M. J. Padgett, S. M. Barnett, S. Franke-Arnold, and J. Courtial, "Measuring the orbital angular momentum of a single photon," *Phys. Rev. Lett.* **88**, 257901 (2002).
21. E. Bolduc, N. Bent, E. Santamato, E. Karimi, and R. W. Boyd, "Exact solution to simultaneous intensity and phase encryption with a single phase-only hologram," *Opt. Lett.* **38**, 3546–3548 (2013).
22. H. Qassim, F. M. Miatto, J. P. Torres, M. J. Padgett, E. Karimi, and R. W. Boyd, "Limitations to the determination of a Laguerre-Gauss spectrum via projective, phase-flattening measurement," *J. Opt. Soc. Am. B* **31**, A20 (2014).
23. A. Baecklund and I. Bengtsson, "Four remarks on spin coherent states," *Phys. Scr.* **T163**, 014012 (2014).
24. P. Kolenderski and R. Demkowicz-Dobrzanski, "Optimal state for keeping reference frames aligned and the platonic solids," *Phys. Rev. A* **78**, 052333 (2008).
25. O. Giraud, P. Braun, and D. Braun, "Quantifying quantumness and the quest for queens of quantumness," *New J. Phys.* **12**, 063005 (2010).
26. J. J. Thomson, "On the structure of the atom: an investigation of the stability and periods of oscillation of a number of corpuscles arranged at equal intervals around the circumference of a circle; with application of the results to the theory of atomic structure," *Philos. Mag. Ser. 6* **7**, 37265 (1904).